HHS Public Access

Author manuscript

Prostate. Author manuscript; available in PMC 2015 October 29.

Published in final edited form as:

Prostate. 2013 May ; 73(7): 778–787. doi:10.1002/pros.22622.

Clinical-Pathologic Correlation Between Transperineal Mapping Biopsies of the Prostate and Three-Dimensional Reconstruction of Prostatectomy Specimens

E. David Crawford[1], **Kyle O. Rove**[1], **Al B. Barqawi**[1], **Paul D. Maroni**[1], **Priya N. Werahera**[2], **Craig A. Baer**[3], **Hari K. Koul**[1], **Cory A. Rove**[4], **M. Scott Lucia**[2], and **Francisco G. La Rosa**[2,*]

[1]Division of Urology, University of Colorado, Anschutz Medical Campus, Aurora, Colorado

[2]Department of Pathology, University of Colorado, Anschutz Medical Campus, Aurora, Colorado

[3]BCSi Incorporated, Colorado Springs, Colorado

[4]Wakely Consulting Group, Englewood, Colorado

Abstract

Background—Extended transrectal ultrasound guided biopsies (TRUSB) of the prostate may not accurately convey true morphometric information and Gleason score (GS) of prostate cancer (PCa) and the clinical use of template-guided (5-mm grid) transperineal mapping biopsies (TPMBs) remains controversial.

Methods—We correlated the clinical-pathologic results of 1,403 TPMB cores obtained from 25 men diagnosed with PCa with 64 cancer lesions found in their corresponding radical prostatectomy (RP) specimens. Special computer models of three-dimensional, whole-mounted radical prostatectomy (3D-WMRP) specimens were generated and used as gold standard to determine tumor morphometric data. Between-sample rates of upgrade and downgrade (highest GS and a novel cumulative GS) and upstage and downstage (laterality) were determined. Lesions ≥ 0.5 cm^3 or GS ≥ 7 were considered clinically significant.

Results—From 64 separate 3D-WMRP lesions, 25 had significant volume (mean 1.13 cm^3) and 39 were insignificant (mean 0.09 cm^3) ($P < 0.0001$); 18/64 lesions were missed by TPMB, but only one was clinically significant with GS-8 (0.02 cm^3). When comparing the cumulative GS of TPMB versus RP, 72% (n = 18) had identical scores, 12% (n = 3) were upgraded, and only 16% (n = 4) were downgraded. Laterality of TPMB and RP was strongly correlated, 80% same laterality, 4% were up-staged, and 16% down-staged.

Conclusions—Our clinical-pathology correlation showed very high accuracy of TPMB with a 5-mm grid template to detect clinically significant PCa lesions as compared with 3D-WMRP, providing physicians and patients with a reliable assessment of grade and stage of disease and the opportunity to choose the most appropriate therapeutic options.

*Correspondence to: Francisco G. La Rosa, MD, University of Colorado Anschutz Medical Campus, Mail Stop 8104, P.O. Box 6511, 12800 East 19th Avenue, Room P18-5124, Aurora, CO 80045-0508. francisco.larosa@ucdenver.edu.

Keywords

prostate cancer; transperineal mapping biopsy; 3D-whole-mount prostatectomy; Gleason score; targeted-focal therapy

Introduction

The diagnosis and treatment of prostatic adenocarcinoma (PCa) has led to a decreasing incidence of advanced stage disease but continues to be a challenge in over-diagnosis and over-treatment [1,2]. Both of these situations can be attributed to the prostate-specific antigen (PSA) era and widespread population screening [3]. Diagnostic tools like transrectal ultrasound guided biopsies (TRUSB) have evolved considerably, resulting in the standard practice of extended 10–12 core biopsy schemes. This has further stimulated the development of a diversity of improved biopsy protocols such as saturation biopsies, super-saturation biopsies, three-dimensional (3D) biopsies, etc., using larger numbers of biopsy cores and different anatomical approaches (transrectal, transurethral, and transperineal) [4]. However, these diagnostic procedures continue to demonstrate significant rates of false negative results when compared with the gold standard radical prostatectomy (RP) specimens, showing important under-staging/grading of disease of up to 30% [4–6]. In addition, patients with strong clinical suspicion of PCa may undergo multiple TRUSB procedures with negative results, suffering anxiety from the uncertainty and delayed diagnosis [7]. Ultimately, these patients present challenging clinical scenarios to the practicing urologist in regard to the discussion of disease outcome, monitoring, and decision-making about the most appropriate treatment [8].

As part of our clinical experience using targeted-focal therapies (TFT) for PCa, a precise map of lesion location must be created in order to stage the real extent of disease. However, TRUSB, used primarily as a diagnostic tool, provides a very partial and limited approximation of Gleason scores (GSs) (GS = primary plus secondary Gleason grades), size and location of PCa lesions, and they cannot be used as a reliable and accurate map for TFT. Because the free hand transrectal approach is relatively limited to the posterior aspect of the prostate, they carry a significant risk of missing relatively small volume high-grade PCa, especially if the lesions are located in the apical and/or anterior regions of the prostate, and for the most part when the gland is enlarged [9–11].

In contrast, template-guided transperineal map ping biopsies (TPMBs) can be used to accurately pin point, measure and grade previously diagnosed PCa, identifying lesions located in areas easily missed by TRUSB. The direct approach to the whole prostate through the perineal region, the systematic sampling guided by a brachytherapy grid template with 5-mm intervals, and live transrectal ultrasound observation of the prostate, ensures coverage of the whole gland regardless of its size. This promises a more precise, 3D representation of location, volume, and extent of the disease [12,13]. Several ex vivo and digital studies have been performed to demonstrate the theoretical accuracy of TPMB. In a previous study, we performed 3D digital reconstructions of autopsy prostates to simulate TPMB and evaluate their accuracy to diagnose clinically significant PCa lesions. The results demonstrated that

the 5-mm grid enabled precise identification of these lesions with sensitivity, specificity, positive predictive value, and negative predictive value of 95%, 30%, 31%, and 95%, respectively [14].

Presently, direct medical experience with TPMB has been limited. To our knowledge, there is not yet a publication correlating results obtained by TPMB in actual clinical conditions with their corresponding three-dimensional reconstructions of whole-mounted radical prostatectomies (3D-WMRP) [15]. We report here the results obtained in a group of men from our clinical practice, most of them initially diagnosed with PCa by means of TRUSB, who were later evaluated with TPMB. Most of these patients were found to have multifocal, higher volume and/or more aggressive disease (higher GS) as compared with their original TRUSB, and they ultimately decided to undergo RP. Based on the high degree of clinical–pathological accuracy in localizing PCa lesions when compared to the gold standard 3D-WMRP, we hypothesize that TPMB can be used as an accurate in vivo staging procedure to detect clinically significant lesions of PCa, providing the physician and the patient with the most appropriate therapeutic options.

Materials and Methods

Patient Selection

This retrospective study was approved by our institutional review board (COMIRB #10-1058). It originally included 32 patients from our clinic between 2006 and 2010 with either histologically proven PCa or strong clinical suspicion. These patients underwent TPMB followed by retropubic RP performed by two surgeons (authors E.D.C. and P.D.M.). We have previously described the TPMB biopsy technique that was performed in this study [16]. Briefly, TPMB was done as a day surgery procedure under conscious sedation in the operative suite. Patients received a dose of pre-operative antibiotics (Ancef 1–2 g IV) within 60 min prior to the procedure, and they were placed in the lithotomy position and injected with local anesthetic into the perineum. An ultrasound transducer was placed in the rectum and a brachytherapy grid with 5-mm spacing was used as a template for biopsy map ping. Fiduciary golden markers were placed midway between the apex and base on either side of the urethra and the coordinates were recorded for future realignment purposes. We captured two-dimensional ultrasound cross-sections at 5 mm increments from apex to base to render 3D in vivo reconstruction of the prostate. Transperineal biopsies were obtained at 5 mm intervals using a standard 18-gauge biopsy gun. Deeper (base) versus shallow (apex) passes at the same grid position were performed to ensure complete base to apex gland coverage. Each biopsy was labeled with their corresponding x–y–z coordinates and placed in separate jars containing 10% buffered formalin for further histopathological analysis. The z coordinate denoted whether the biopsy was taken at the apex or the base of the prostate.

Most patients included a prior diagnosis of low-grade (GS ≤ 6) or intermediate grade (GS-7) PCa, with low-volume (≤2 positive cores), as diagnosed via TRUSB. RP was considered for these patients on the basis of findings at TPMB (multifocality and/or higher volume, and/or more aggressive disease with higher GS) or patient preference. No patient was excluded for prostate size or inaccessibility. During patient selection, seven were excluded from analysis, as five had surgery at outside hospitals, and two could not be accurately evaluated due to

neoadjuvant hormonal therapy changes [17,18]. Thus, 25 patients were included in the final analysis.

Pathology Review

Pathology review of TRUSB was performed in 8 of the 25 patients in our institution and read by one of our uropathologists (authors F.L.R. or M.S.L.); the remaining 17 was performed outside our institution in different private pathology laboratories from which nine were re-read as second opinion diagnosis by one of the above uropathologists.

Pathology review of TPMB was performed in six of the 25 patients in our institution and read by one of our uropathologists; the remaining 19 were performed outside our institution in an outside specialized uropathology laboratory (Bostwick Laboratories, Glen Allen, VA).

All specimens interpreted by our uropathologists were graded according to the 2005 International Society of Urological Pathology modified Gleason system.

Overall GS was assigned based on highest score in the set. However, the increased sampling density (granularity) inherent to the TPMB technique was recognized to lead to oversampling of higher-grade areas, leaving the pathologists with biased results from single needle sample. Thus if one is to assign an overall grade to a cohort of TPMB, one is necessarily biased to the core with the highest grade cancer, which may not represent the overall distribution of Gleason grades within the prostate at RP. For this reason, we used a cumulative GS for TPMB to better reflect individual grades amongst the entire cohort of positive biopsies for a single patient. Primary and secondary Gleason grades of each positive biopsy core were identified and counts of each grade were tabulated to arrive at an overall revised grade. The two most common grades seen amongst all positive biopsies in a single TPMB cohort were then summed to arrive at a cumulative GS.

An example illustrates this calculation: If a TPMB set had three PCa positive biopsy cores, consisting of Gleason grades 3 + 3, 4 + 4, and 3 + 3, the conventional overall grading (highest score) would be GS-8, indicating an aggressive disease. If one were to separate out the individual Gleason grades across all the positive biopsies (3, 3, 4, 4, 3, 3), and count the respective number of individual grade occurrences (four 3s and two 4s), one arrives at a cumulative GS of 3 + 4 (GS-7). This narrower approximation of an overall GS was used in an additional analysis to compare TPMB to 3D-WMRP.

All whole prostatectomy specimens were fixed in 10% buffered formalin, sectioned at 4 mm intervals from apex to base and entirely submitted for paraffin embedding and staining as previously described [19,20]. Pathology evaluations of prostatectomy sections were blinded to TRUSB or TPMB results. GS was assigned to each individual PCa lesion in prostatectomy specimens based on the primary and secondary Gleason grades [21].

Coordinates of positive and negative biopsy (x–y– z, as recorded at the time of TPMB procedure) were mapped on a two-dimensional grid (Fig. 1). In some patients, dynamic three-dimensional reconstructions, integrating TPMB pathology results with serial (apex to base) two-dimensional transrectal ultrasound images, obtained at the time of the TPMB procedure, were examined (Fig. 2).

In all cases, drawings of prostatectomy slices containing tumor and urethra outlines were digitized (Fig. 3) using a Wacom LCD Tablet, Cintiq model DTZ-1200W (Wacom, Co. Ltd., Tokyo, Japan) into Adobe Photoshop CS2 software (Adobe Systems Inc., San Jose, CA). Using these digitized sections, dynamic 3D computer models of each RP specimen were generated with software developed at our institution and then visualized for analysis (Fig. 4) with MRIcro soft ware (Georgia Institute of Technology, Atlanta, GA) [22]. These reconstructions were used to determine tumor morphometric data including multifocality, laterality, volume, surgical margins, and extraprostatic extension with corresponding identification of GS.

The independent histopathology TPMB and prostatectomy results were compared. For TPMB, a lesion was defined as any discrete set of contiguous positive biopsy locations on 5-mm grid points (side by side or diagonal). On 3D-WMRP, our 3D reconstruction algorithm identified discrete lesions using rules based on proximity, connectivity, and corresponding GS. For each 3D-WMRP lesion, a corresponding lesion was noted to be either present or absent on TPMB, as determined by consensus between two authors (K.O.R. and P.D.M.). Sub-analyses were also performed to determine ability for TPMB to accurately detect all lesions by laterality, regardless of size or GS. Lesions that overlapped midline were judged, by consensus, based on predominant appearance to be located in one subsection, another, or both. 3D-WMRP lesions were further classified according to Epstein's criteria, in which lesions with volumes ≥ 0.5 cm^3 or GS ≥ 7 were considered clinically significant [5].

Statistical Analysis

We defined four possible transitions between TPMB and 3D-WMRP, including upgrade or downgrade of GS (e.g., GS-7 to GS-6), and upstage or down stage based on laterality (e.g., unilateral to bilateral) Descriptive statistics are reported with median values (range). All statistical tests were two-sided, and *P*-values <0.05 were considered statistically significant.

Results

Clinical Analysis

The 25 selected patients underwent TPMB, subsequent RP and data analysis. Twenty-two of these patients presented with a prior histopathological diagnosis of PCa on TRUSB. One patient presented with PCa (GS-6) in 2 of 59 chips of a previous transurethral resection. Two other patients had strong clinical suspicions of PCa, but each had one or more negative prior TRUSB performed outside our institution. Patient demographics and characteristic findings on TPMB and 3D-WMRP are provided in Table I. The study patients' median age was 66 years, median PSA was 5.1 ng/ml, and median prostate volume was 32 cm^3 measured by ultrasound at TPMB.

Pathology Analysis

Total number of cores on TRUSB was 303 with a median number of 12 per patient (range 9-25); for the purpose of this study and because of limited information of TRUSB results, only Gleason grade and scores were analyzed. The total number of cores on TPMB was 1,403 with a median number of 49 per patient (range 27–110 cores); the number of TPMB

cores depended on the shape and size of the prostate gland under ultrasound examination. The median number of positive TPMB cores was 8 per patient (range 0–31). The median number of lesions on 3D-WMRP per patient, irrespective of clinical significance, was 2 (range 0–7) (Table II).

Clinical-Pathologic Correlations

Among all patients, a total of 64 lesions were identified on WMRP specimens; from these, 25 were considered to be clinically significant (≥0.5 cm^3 or GS ≥ 7). TPMB did not identify 18 of 64 lesions found at 3D-WMRP, but only one lesion was considered to be clinically significant, corresponding to a GS-8, small volume (0.02 cm^3) lesion in a patient with two other significant lesions that were properly identified by TPMB. Mean volume (±SEM) of clinically significant lesions as measured by 3D-WMRP was 1.13 ± 0.26 cm^3 versus 0.09 ± 0.02 cm^3 for insignificant lesions. These volumes were significantly different ($P < 0.0001$). Table III provides further breakdown of GS by patients across histopathologic data sets.

When comparing GS of TRUSB to 3D-WMRP, 40% had no change, 8% were downgraded, and 52% were upgraded. Comparison of highest GS between TPMB versus 3D-WMRP demonstrated no significant differences in variance (folded *F*-test: $P = 0.329$). When examining highest GS among all positive TPMB, GS-6 constituted 32%, GS-7 was 40%, and GS-8 was 24%. Based on histopathological findings, 56% of 3D-WMRP had GS that matched their corresponding TPMB (Fig. 5), 36% of patients were downgraded and 8% were upgraded. A breakdown of the downgrading activity is as follows: 4 + 4 to 3 + 4 (5% or 20%); 4 + 3 to 3 + 3 (1% or 4%); and 3 + 4 to 3 + 3 (3% or 12%). One of 25 patients (4%) at TPMB was found to be negative for PCa. Despite the negative results and considerable counseling, this patient's preference was surgical resection; the 3D-WMRP of this patient was also found to be negative.

When examining cumulative GS among all TPMB, GS-6 accounted for 32% of the population and GS-7 accounted for 64%. Using these cumulative GS (in contrast to using only the overall or highest GS), up to 72% (n = 18) had identical scores, 12% (n = 3) were upgraded, and only 16% (n = 4) were downgraded (3 + 4 to 3 + 3). Thus, the calculation of cumulative GS correctly predicted the final GS in 5 additional patients who had been previously downgraded, and correctly identified an additional single patient who was previously upgraded.

When comparing the laterality of PCa lesions determined by TPMB, 80% (n = 20) had agreement with histopathological findings of 3D-WMRP, 16% of patients were down-staged, and the remainder were up-staged. However, only 36% of patients had both GS and laterality of TPMB match with histopathological findings of their corresponding 3D-WMRP. Figure 6 shows a Venn diagram demonstrating the rates of upstage, upgrade, downstage, and down grade for men with positive TPMB.

As stated before, two patients presented with prior negative TRUSB and elevated PSA values of 8.3 and 10.0 ng/ml. The first had a total of 50 cores at TPMB with two positive biopsies, each GS-6. At 3D-WMRP, three lesions were noted, none of which were clinically significant. Each was GS-6 and they were 0.02, 0.02, and 0.01 cm in volume. The second of

these two patients had 46 total TPMB cores with 8 positive cores, six of which were GS-7, and one GS-8. Three separate lesions were discovered on 3D-WMRP (GS-7, GS-8, and GS-8, and with volumes of 1.46, 0.02, and 0.16 cm respectively). Two of these three lesions were seen at TPMB, and the one missed (GS-8, 0.02 cm^3) had no additional clinical value in this case since the TPMB had already detected other two additional clinically significant lesions.

Discussion

The main goal of this study is to demonstrate the clinical-pathologic correlation between TPMB and WMRP. The statistical power of our study lies on the number of TPMB specimens (1,403 biopsy cores) able to detect the 64 cancer lesions observed in the gold standard RP specimens. This preliminary but important patient experience reflects a single tertiary-care institution, and selection bias is reflected by patients who were highly motivated, seeking better staging for newly diagnosed disease. Nevertheless, we consider that the number of patients does not interfere with our final analysis and interpretation. This study is focused on the ability of TPMB to better identify and stage in vivo the presence of PCa lesions and does not pretend to determine the effect of further staging of disease on clinical outcomes. In addition, the complex requirements for this type of study make it difficult to gather a larger number of cases; namely, the simultaneous conditions of histologically proven PCa on TRUSB, followed by TPMB and eventual RP. Nevertheless, this selected group of patients provided us a unique opportunity to perform a clinical-pathologic comparison of TPMB versus 3D-WMRP specimens. All patients diagnosed with PCa by TRUSB were found to have upgraded disease status after TPMB, warranting radical surgery.

Accurate grade and stage of PCa is required to tailor therapeutic regimens to individual patients. A possible constraint in the interpretation of our results could be the fact that most of the TPMB (19 of 25) were graded by an outside uropathology laboratory (Bostwick's) and the grading of the WMRP were done by our in-house uropathologists. However, in past interactions with this laboratory, we have found no significant interobserver variability between our GS results. If a significant interobserver variability had been present, our data would have been biased towards the null, and against our hypothesis and conclusions. Thus, we consider that this issue was negligible.

The results presented here demonstrate the potential for TPMB to significantly improve the scope for PCa diagnosis upon the results obtained with extended TRUSB. TPMB detected practically all clinically significant tumors found in the gold-standard 3D-WMRP specimens. These clinical-pathologic data confirms our previous observation done on a computer simulation model with autopsy specimens, which demonstrated the potential of a 5-mm grid TPMB to diagnose significant disease with very high sensitivity (95%) and at the same time indicated absence of significant disease with very high negative predictive value (95%) [14]. In that same study we compared the efficacy of a 10-mm grid and found that doubling the spacing of the prostate sampling misses clinically significant lesions, decreasing accuracy regarding GS and laterality. In our current study, we decided to determine the performance of a hypothetical 10-mm grid by removing the pathology results

of every other grid point on the existing 5-mm grid data for this cohort of patients. Overall, if a 10-mm grid had been used, we noted a reduced median of 12 cores per patient (range 6–30) with only two positive cores (range 0–8) per patient. In five patients, staging biopsies using a 10-mm grid would have been falsely negative, and four clinically significant lesions would have otherwise been missed. In total, a full 60% or 15 patients would have been upgraded, upstaged or both. Thus, the current TPMB evaluation using a 5 mm grid has a high degree of clinical–pathological accuracy for identifying GS, focality, size and laterality of the disease.

While our definition of clinical significance was dependent on individual cancer foci GS and volume, total tumor burden may represent another measure of significance. This was demonstrated with one individual in this series with seven lesions on 3D-WMRP, each GS-6 ranging from 0.01 to 0.12 cm^3 in volume but totaling 0.44 cm^3.

The observed 36% rate of downgrade from TPMB to 3D-WMRP is higher than expected. This can be explained by the use of the classic overall, highest GS within a set of positive biopsies of a TPMB. TPMB inherently provides increased sampling density or granularity, thus leading to potentially better sampling of small areas of higher-grade disease within the prostate. If one probe samples an area with only Gleason grade 4, it will necessarily be reported as 4 + 4 (GS-8). But as we found in many cases, surrounding biopsies would often be positive for Gleason grade 3 and the final pathology on 3D-WMRP would be either 3 + 4 (GS-7) or 4 + 3 (GS-7). As such, the single GS-8 biopsy at TPMB would bias the results (nearly half of the downgrades occurred from GS-8 to GS-7). For this reason, we completed a separate analysis with a different TPMB grading interpretation, which we termed “cumulative GS” that accounts for the statistical granularity of data provided by TPMB and correlates better with the gold-standard 3D-WMRP pathology results. Using the highest GS at TPMB necessarily biases the interpretation to worse pathology results depending on one or more biopsies that may have sampled the same cancer area. We consider that sampling in a single core at TPMB should not bias the overall interpretation of disease burden. Thus, using the cumulative GS minimizes the bias of using highest GS and maintains the fidelity of this staging tool by adjusting to the results of the gold standard. Using this methodology, upgrading from TPMB to 3D-WMRP increased slightly to 12% (from 8%) and downgrading decreased dramatically from 36% to 16%. We must caution, however, that this alternative scoring system must be further evaluated and modified by evaluating a larger number of patients to better determine scoring cutoffs.

To date, the primary obstacle in identifying appropriate patients for targeted treatments has been the inability to fully characterize a patient's disease status (stage) and topographic location of cancer lesions. While saturation TRUSB may appear to be a good approach for improved diagnosis of disease, particularly in patients with prior negative extended TRUSB, the standardization of more accurate mapping procedures to evaluate patients considering TFT remains a difficult task. A recent study found saturation TRUSB and transperineal saturation rebiopsy to have similar PCa detection rates (26% vs. 31%), highlighting the limitations of 12-core TRUSB protocols in some patients. Some protocols using a limited version of TPMB such as the one reported by Abdollah et al. [25] did not consider prostate volume as an important statistical variant; they only used a fixed number of biopsy cores per

patient and did not employ a grid. In contrast, the TPMB using a 5-mm grid aided by ultrasound imaging of the prostate is particularly unique as it standardizes the number of cores obtained per patient based on unit of prostate volume, improving the uniformity of gland coverage. This is further enhanced by the integrated digital 3D reconstruction of pathology results with ultrasound images leading to more accurate staging and localization of the disease. This procedure can help the physician and patient to select the most appropriate therapy in function of the stage of the disease, ranging from more conservative approaches (TFT) in cases of localized and/or low grade disease to those that require more radical treatment (prostatectomy) due to multifocal and/or high grade disease [26].

Comparison of TPMB and 3D-WMRP was subject to possible errors in registration of the histopathology sets and difficulty identifying urethra on TPMB. Due to the relatively limited number of patients in this study, differentiation of Gleason grades in the GS-7 group (3 + 4 vs. 4 + 3) was not performed. Furthermore, the evaluation of cumulative GS for TPMB represents an improved estimation over the traditional overall, highest GS comparisons, and further volumetric studies could provide a more accurate GS assessment of TPMB.

Finally, there is a higher cost associated with the choice of the 5-mm grid at TPMB due to the procedure itself as for the large number of biopsy cores to be processed in a pathology laboratory. Thus, cost-effectiveness analysis and quality of life outcomes after TPMB should be performed to understand the implications of utilizing this staging tool.

Conclusion

We know from several large studies that under-and over-grading associated with TRUSB protocols can lead to a significant risk for nonmatching treatment [27,28]. In contrast, the accuracy of the 5-mm grid TPMB to detect clinically significant cancer lesions provides clinicians and patients with more reliable information in order to choose the most appropriate treatment. TPMB with a 5-mm grid template closely reflects true PCa disease state as found at RP. Thus, we consider that, in selected patients, TPMB is an important staging tool that better informs and reassures clinicians and patients alike as to the true stage of their disease. TPMB can detect or rule out more aggressive disease, identifying with more accuracy the GS and size of PCa lesions, ensuring that patients are not mistakenly under-treated or unnecessarily over-treated, minimizing therapy-related morbidity.

Acknowledgments

The authors would like to thank the laboratory technicians who made possible the fine histological preparations used in this work: Kathy Lux, Erin Genova, and Nancy Dunscomb from the Prostate Diagnostic Laboratory, University of Colorado Anschutz Medical Campus.

References

1. Ung JO, Richie JP, Chen MH, Renshaw AA, D'Amico AV. Evolution of the presentation and pathologic and biochemical outcomes after radical prostatectomy for patients with clinically localized prostate cancer diagnosed during the PSA era. Urology. 2002; 60:458–463. [PubMed: 12350484]

2. Draisma G, Etzioni R, Tsodikov A, Mariotto A, Wever E, Gulati R, Feuer E, de Koning H. Lead time and overdiagnosis in prostate-specific antigen screening: Importance of methods and context. J Natl Cancer Inst. 2009; 101:374–383. [PubMed: 19276453]

3. Barry MJ. Screening for prostate cancer—The controversy that refuses to die. N Engl J Med. 2009; 360:1351–1354. [PubMed: 19297564]

4. Chun FK, Epstein JI, Ficarra V, Freedland SJ, Montironi R, Montorsi F, Shariat SF, Schro¨der FH, Scattoni V. Optimizing performance and interpretation of prostate biopsy: A critical analysis of the literature. Eur Urol. 2010; 58:851–864. [PubMed: 20884114]

5. Epstein JI, Walsh PC, Carter HB. Importance of posterolateral needle biopsies in the detection of prostate cancer. Urology. 2001; 57:1112–1116. [PubMed: 11377320]

6. Rabets J, Jones JS, Patel A, Zippe CD. Prostate cancer detection with office-based saturation biopsy in a repeat biopsy population. J Urol. 2004; 172:94–97. [PubMed: 15201745]

7. Andriole GL. The lottery of conventional prostate biopsy. Nat Rev Urol. 2009; 6:188–189. [PubMed: 19352393]

8. Jones JS. Management of rising prostate specific antigen following a negative biopsy. Cur Opin Urol. 2010; 20:198–203.

9. Onik G, Vaughan D, Lotenfoe R, Dineen M, Brady J. The ‘male lumpectomy’: Focal therapy for prostate cancer using cryoablation results in 48 patients with at least 2-year follow-up. Urol Oncol. 2008; 26:500–505. [PubMed: 18774463]

10. Blana A, Murat FJ, Walter B, Thuroff S, Wieland WF, Chaussy C, Gelet A. First analysis of the long-term results with transrectal HIFU in patients with localized prostate cancer. Eur Urol. 2008; 53:1194–1201. [PubMed: 17997026]

11. Ahmed HU, Emberton M. Benchmarks for success in focal therapy of prostate cancer: Cure or control? World J Urol. 2010; 28:577–582. [PubMed: 20830476]

12. Onik G, Miessau M, Bostwick DG. Three-dimensional prostate mapping biopsy has a potentially significant impact on prostate cancer management. J Clin Oncol. 2009; 27:4321–4326. [PubMed: 19652073]

13. Barzell WE, Melamed MR. Appropriate patient selection in the focal treatment of prostate cancer: The role of transperineal 3-dimensional pathologic mapping of the prostate–A 4-year experience. Urology. 2007; 70:S27–S35.

14. Crawford ED, Wilson SS, Torkko KC, Hirano D, Stewart JS, Brammell C, Wilson RS, Kawata N, Sullivan H, Lucia MS, Werahera PN. Clinical staging of prostate cancer: A computer-simulated study of transperineal prostate biopsy. BJU Int. 2005; 96:999–1004. [PubMed: 16225516]

15. Hu Y, Ahmed HU, Carter T, Arumainayagam N, Lecornet E, Barzell W, Freeman A, Nevoux P, Hawkes DJ, Villers A, Emberton M, Barratt DC. A biopsy simulation study to assess the accuracy of several transrectal ultrasonography (TRUS)-biopsy strategies compared with template prostate mapping biopsies in patients who have undergone radical prostatectomy. BJU Int. 2012; 110:812–820. [PubMed: 22394583]

16. Barqawi AB, O'Donnell CI, Siomos VJ, Hou AH. The effect of short-term dutasteride intake in early-stage prostate cancer: Analysis of 148 patients who underwent three-dimensional prostate mapping biopsy. Urology. 2010; 76:1067–1071. [PubMed: 20472268]

17. Civantos F, Soloway MS, Pinto JE. Histopathological effects of androgen deprivation in prostatic cancer. Semin Urol Oncol. 1996; 14:22–31. [PubMed: 8725888]

18. Reuter VE. Pathological changes in benign and malignant prostatic tissue following androgen deprivation therapy. Urology. 1997; 49:16–22. [PubMed: 9123731]

19. Miller GJ, Cygan JM. Morphology of prostate cancer: The effect of multifocality on histological grade, tumor volume and capsule penetration. J Urol. 1994; 152:1709–1713. [PubMed: 7933231]

20. Westra, WH.; Hruban, RH.; Phelps, TH.; Isacson, C., editors. Surgical pathology dissection: An illustrated guide. 2nd. New York, NY: Springer-Verlag New York Inc.; 2003.

21. Gleason DF. Histologic grading of prostate cancer: A perspective. Hum Pathol. 1992; 23:273–279. [PubMed: 1555838]

22. Werahera PN, Miller GJ, Torkko K, Crawford ED, Stewart JS, Deantoni EP, Miller HL, Lucia MS. Biomorphometric analysis of human prostatic carcinoma using three dimensional com puter models. Hum Pathol. 2004; 35:798–807. [PubMed: 15257542]

23. Walz J, Graefen M, Chun FK, Erbersdobler A, Haese A, Steuber T, Schlomm T, Huland H, Karakiewicz PI. High incidence of prostate cancer detected by saturation biopsy after previous negative biopsy series. Eur Urol. 2006; 50:498–505. [PubMed: 16631303]

24. Barqawi AB, Rove KO, Gholizadeh S, O'Donnell CI, Koul H, Crawford ED. The role of 3-dimensional mapping biopsy in decision making for treatment of apparent early-stage prostate cancer. J Urol. 2011; 186:80–85. [PubMed: 21571335]

25. Abdollah F, Novara G, Briganti A, Scattoni V, Raber M, Roscigno M, Suardi N, Gallina A, Artibani W, Ficarra V, Cestari A, Guazzoni G, Rigatti P, Montorsi F. Trans-rectal versus trans-perineal saturation rebiopsy of the prostate: Is there a dif ference in cancer detection rate? Urology. 2011; 77:921–925. [PubMed: 21131034]

26. Coogan CL, Latchamsetty KC, Greenfield J, Corman JM, Lynch B, Porter CR. Increasing the number of biopsy cores improves the concordance of biopsy Gleason score to prostatectomy Gleason score. BJU Int. 2005; 96:324–327. [PubMed: 16042723]

27. Cam K, Yucel S, Turkeri L, Akdas A. Accuracy of transrectal ultrasound guided prostate biopsy: Histopathological correla tion to matched prostatectomy specimens. Int J Urol. 2002; 9:257–260. [PubMed: 12060438]

28. Sinnott M, Falzarano SM, Hernandez AV, Jones JS, Klein EA, Zhou M, Magi-Galluzzi C. Discrepancy in prostate cancer localization between biopsy and prostatectomy specimens in patients with unilateral positive biopsy: Implications for focal therapy. Prostate. 2012; 72(11): 1179–1186. [PubMed: 22161896]

Abbreviations

PCa	prostate cancer
PSA	prostate-specific antigen
TRUSB	transrectal ultrasound guided biopsies
TPMB	transperineal mapping biopsies
RP	radical prostatectomy
WMRP	whole-mounted radical prostatectomy
3D-WMRP	three-dimensional whole-mounted radical prostatectomy
TFT	targeted-focal therapy

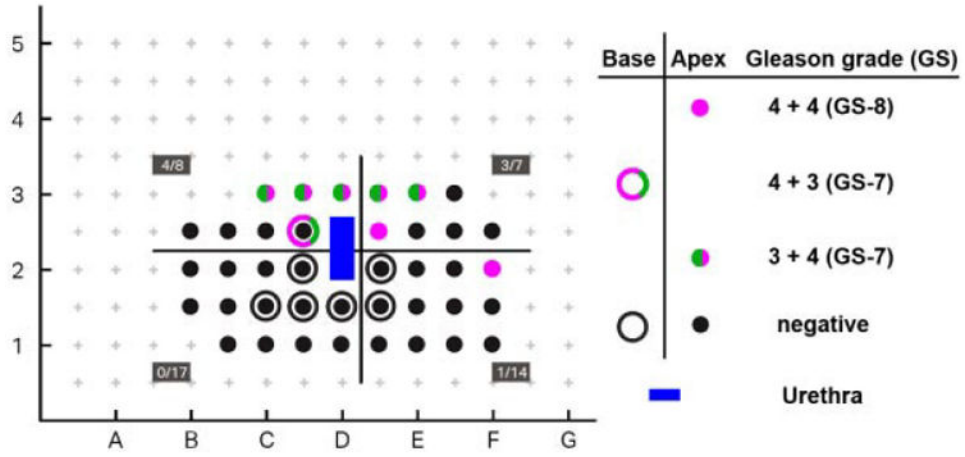

Fig. 1.

Two-dimensional, schematic representation of pathology results from transperineal mapping biopsies (TPMBs) in a patient who had a total of 46 biopsies obtained with an18-gauge biopsy gun. Results are plotted in their corresponding x and y positions in relationship to a brachy therapy grid with 5 -mm spacing used for biopsy mapping. The z positions are represented as outlined circles (deep or base) and solid circles (proximal or apex). Gleason grades are depicted in green for Gleason grade 3 and purple for Gleason grade 4. Positive biopsies were: Five with Gleason grades 3 + 4 (GS-7), one with Gleason grade 4 + 3 (GS-7), and two with Gleason grade 4 + 4 (GS-8). One cluster of positive biopsies (Gleason grades 3 and 4) is observed at the right-mid and anterior aspect of the prostate and another distinct lesion (Gleason grade 4 + 4, GS-8) at left lateral. The blue area (not sampled) corresponds to the urethra at the middle of the set of biopsies at grids D2 andD2.5.

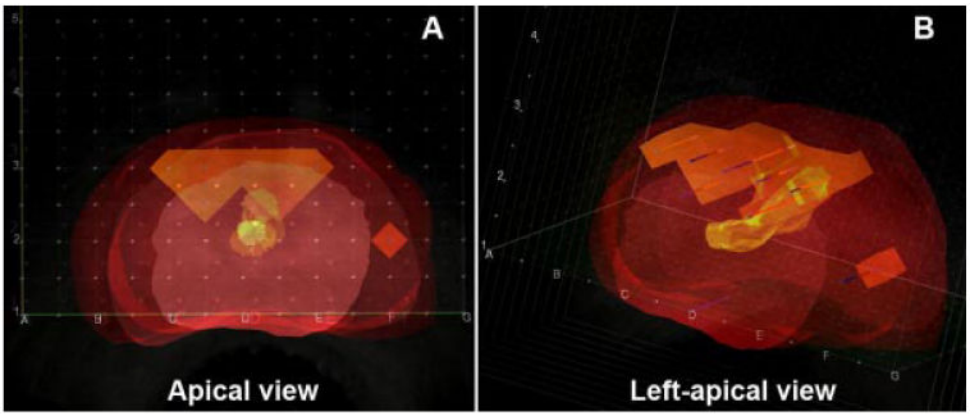

Fig. 2.

Screen captures from adynamic three-dimensional reconstruction of transrectal ultrasound images obtained during the transperineal mapping biopsy procedure from the same patient in Figure 1. The pathology results with cancer lesions have been also inserted in their corresponding x–y–z locations identifying the two distinct lesions described in Figure 1: (**A**) Apical view with the same perspective as depicted in Figure 1. **B**: Let-apical view of the same specimen showing the anterior-posterior extension of the cancer lesions.

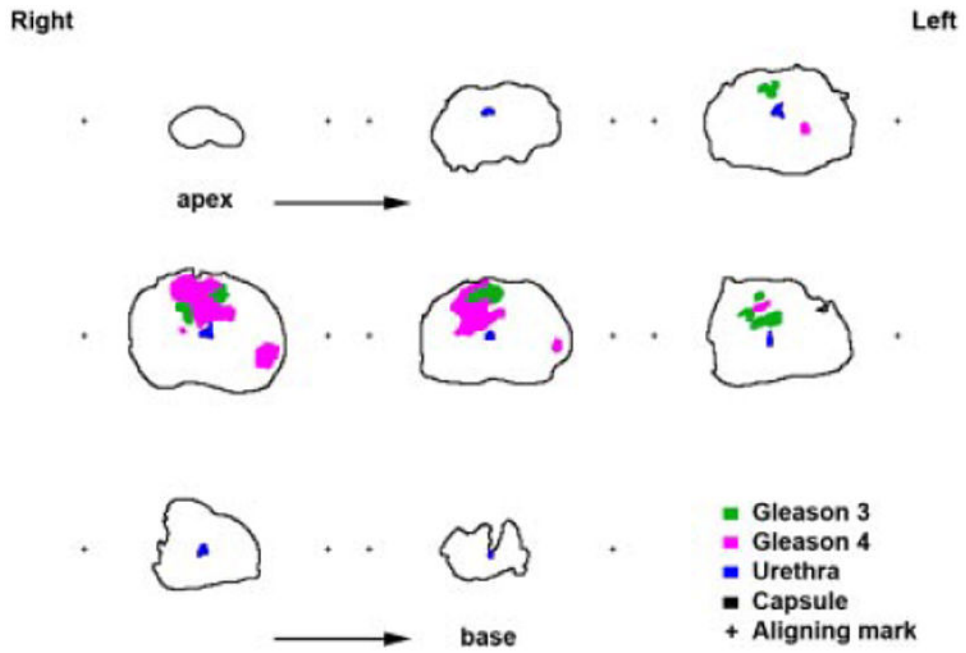

Fig. 3.

Digital outline drawings obtained from the whole mount prostatectomy slides at 4 -mm increment, from ape× (upper right) to base (lower left). Cancer lesions have been mapped under the microscope and identified in green for Gleason 3 and purple for Gleason 4; urethra (blue), capsule (black), and aligning marks (+) are alsorepresented.

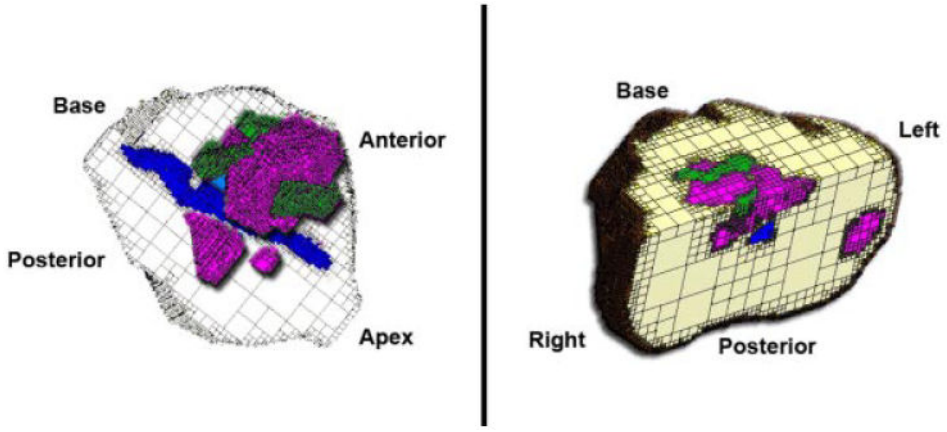

Fig. 4.

Using the digitized images from the map in Figure 3, a dynamic 3D computer model was generated with software developed at our institution and then visualized for analysis with MRIcro software. Color coding are the same as in Figures 1 and 3. These reconstructions were used to determine tumor morphometric data, including multifocality, laterality, volume, surgical margins, and extraprostatic extension with corresponding GS. The screen captures shown here, as compared with the data and images from the transperineal mapping biopsies illustrated in Figures 1 and 2, show equivalent tumor morphometric data, including multifocality, laterality, and volumes, as well as their relationship with urethra and surgical margins.

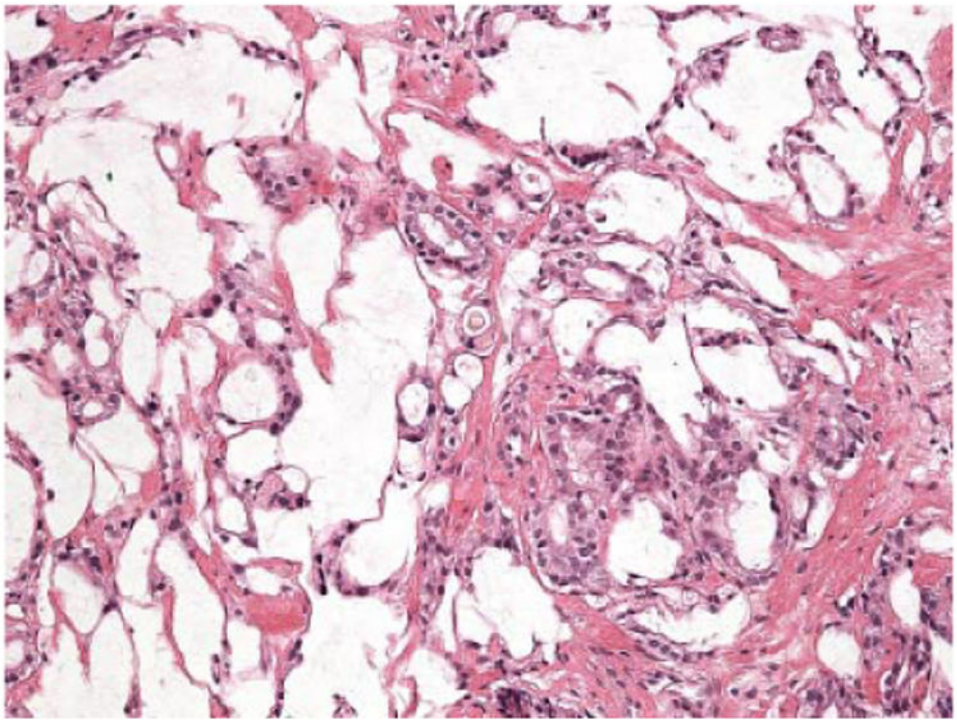

Fig. 5.

Representative image (20× objective) of the focus of prostatic adenocarcinoma Gleason grade 4 + 4 (GS-8) found in the lesion located at the left-peripheral area of the prostate presented in Figures 1–4. Both, transperineal biopsy and the whole-mounted radical prostatectomy specimens showed the same tumor histology.

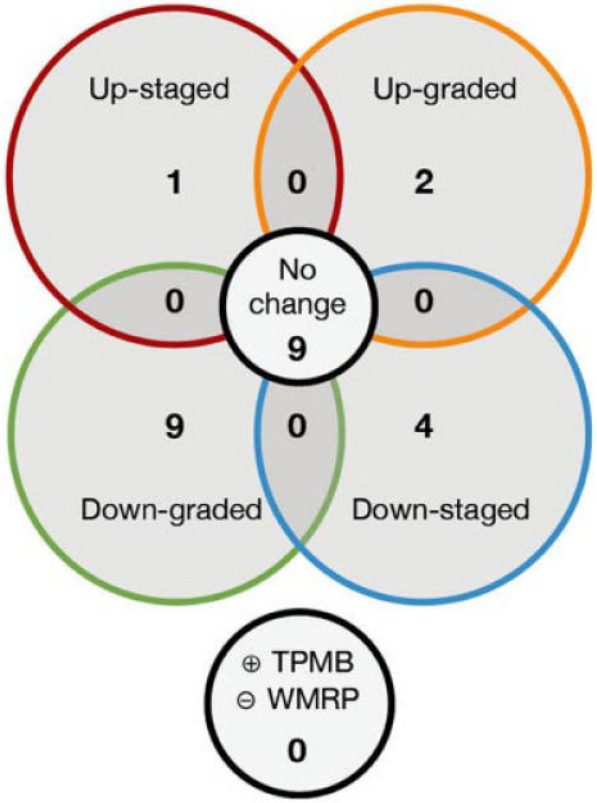

Fig. 6.

Venn-diagram representation of activity of patients between positive results from transperineal mapping biopsies (TPMBs) and three-dimensional whole-mounted radical prostatectomies (3D-WMRP). One patient is not included here as hisTPMB and 3D-WMRP were both negative. (+) indicates presence of prostatic cancer, and (−) indicates no cancer.

Table I

Study Population Characteristics

Demographics	
Patients (n)	25
Age (years)	66 (49–73)
Median PSA (ng/ml)	5.0 (1.0–10.0)
Prostate volume (cm^3)	32 (20–63)
Transperineal mapping biopsy (TPMB)	
Total cores per patient	49 (27–110)
Positive cores per patient	8 (0–31)
Distinct lesions per patient	3 (0–5)
Total lesions detected in population	64
Time from TRUSB to TPMB (days)	126 (60–528)
Three-dimensional whole-mounted radical prostatectomy (3D-WMRP)	
Lesions per patient	2 (0–7)
Total lesions detected in population	64 (no exactly the same lesions as TPMB)
Mean lesion volume (cm^3 ± SEM)	0.50 ± 0.12
Significant lesion volume (n = 25)	1.13 ± 0.26
Insignificant lesion volume (n = 39)	0.09 ± 0.02

All values are given as median (range), except where indicated. Lesion significance was determined by individual lesion volumes ≥ 0.5 cm^3 or GS ≥ 7.

Table II

Histological Findings of Transperineal Mapping Biopsies (TPMB) Versus Three-dimensional Whole-mounted Radical Prostatectomy (3D-WMRP) Specimens

	TPMB	3D-WMRP
Lesions per patient	3 (0–5)	2 (0–7)
Total number of cancer lesions	64	64
Significant		25
Insignificant		39
Lymph nodes		(+) 0/(×) 10/(−) 15
Surgical margins		(+) 7/(−) 18
Extraprostatic extension		(+) 0/(−) 25
Seminal vesicles		(+) 0/(−) 25

Range is shown in parentheses where appropriate. (+) Denotes positive status, (×) denotes none found or evaluated, and (−) denotes negative status.

Table III

Patient Distribution by Gleason Scores (GS) According to Transperineal Mapping Biopsy (TPMB) and Three-dimensional Whole-Mounted Radical Prostatec tomy (3D-WMRP)

Gleason score (GS)	TPMB (highest)	TPMB (cumulative)	3D-WMRP (highest)
GS-6	8	8	10
GS-7	10	16	13
GS-8	6	0	1
Negative	1[a]	1[a]	1[a]

TPMB (highest) refers to the highest GS seen in any one biopsy for a single patient. TPMB (cumulative) refers to the cumulative sum GS, arrived at by adding the total number of any one Gleason grade across all positive biopsies and then determining the overall most common primary and secondary Gleason grades, and summing them.

[a]The negative TPMB and 3D-WMRP reflect the same patient who originally presented with GS-6 in 2 of 59 chips from trans urethral resection of the prostate. (+) denotes positive status, (×) denotes none found or evaluated, and (−) denotes negative status.